WHERE DO WE STAND WITH SUPERSYMMETRIC CANDIDATES FOR DARK MATTER?

A. BOTTINO
Dipartimento di Fisica Teorica, Università di Torino
and INFN, Sez. di Torino, Via P. Giuria 1, I–10125 Torino, Italy
E-mail: bottino@to.infn.it

ABSTRACT

We first briefly recall the generic features of relic neutralinos, as may be derived in supersymmetric models, only constrained by accelerator bounds. Then we report the main results of an investigation carried out with Belli, Bernabei, Donato, Fornengo, Prosperi and Scopel on the possible implications for relic neutralinos of an annual–modulation effect singled out by the DAMA/NaI experiment of WIMP direct search. The annual–modulation region discussed in the present report takes into account uncertainties in the galactic astrophysical velocities and entails, for the neutralino mass, the range 30 GeV $\lesssim m_\chi \lesssim$ 130 GeV (at 1–σ C.L.), with a further extension in the upper bound, when a possible bulk rotation of the dark matter halo is taken into account. It is shown that these data are consistent with a relic neutralino as a dominant component of cold dark matter (on the average in our universe and in our galactic halo). We also discuss the features of the relevant supersymmetric configurations in connection with the discovery potential of the accelerators of the present generation.

1. Introduction

Extensive investigations have been carried out on supersymmetric particles as possible candidates for Cold Dark Matter (CDM) [1]. This, indeed, for very good reasons. In fact, the Lightest Supersymmetric Particle (LSP), under the condition that the R–parity is conserved, would be stable; furthermore, in extended regions of the supersymmetric parameter space this LPS would turn out to be weakly interacting, and would entail a significant contribution to the matter density in the Universe, at a level required by current local and cosmological observations. A supersymmetric particle which would meet these requirements for being a Weakly Interacting Massive Particle (WIMP) is the neutralino, the lowest–mass linear superposition of photino ($\tilde{\gamma}$), zino ($\tilde{Z}$) and the two higgsino states ($\tilde{H}_1^\circ$, $\tilde{H}_2^\circ$) [2]

$$\chi \equiv a_1\tilde{\gamma} + a_2\tilde{Z} + a_3\tilde{H}_1^\circ + a_4\tilde{H}_2^\circ \,. \tag{1}$$

(hereafter the neutralino is called a *gaugino*, when $P > 0.9$, is called *mixed* when $0.1 \leq P \leq 0.9$ and a *higgsino* when $P < 0.1$, P being defined as $P \equiv a_1^2 + a_2^2$).

Further noticeable features of a relic neutralino are that this particle, at variance with some of the other dark matter candidates, may give rise to measurable detection rates in direct as well as indirect searches for WIMPs [1].

The main properties of relic neutralinos have been investigated in great detail in various supersymmetric schemes, from the simple Minimal Supersymmetric extension of the Standard Model (MSSM) to the more sophisticated supergravity-inspired models [2]. An indication about the strong interest in relic neutralinos as dark matter

candidates is, for instance, provided by the recent theoretical papers which pursue the investigation of the various ways of searching for exotic signatures of their annihilation. Improved evaluations and new ideas have, for example, been developed for exotic components of cosmic rays, due to neutralino annihilation in the halo: antiprotons [3], antideuterons [4], positrons [5], photons [6], and for the neutrinos produced by annihilation inside the Earth (see the suggestion [7] about a new population of low-energy neutralinos which could sizeably enhance the signal [8]).

However, it has to be noted that the theoretical evaluations of various relevant quantities, relic abundance and detection rates, are unavoidably spread over extremely wide ranges, since no specific hints about realization of supersymmetric theories in nature are available yet. Indeed, from accelerator data we have at our disposal only constraints about the parameters entering in our supersymmetric theoretical schemes. An example of this situation is provided by Fig.1, which displays the neutralino relic abundance $\Omega_\chi\, h^2$ (Ω_χ is the neutralino matter density in units of the critical density and h is the Hubble constant in units of 100 km s^{-1} Mpc^{-1}) versus the neutralino mass m_χ. The values plotted in Fig.1 were obtained in a generic MSSM scheme, whose details will be given in Sect. III. One notices that the values of the neutralino relic abundance spread over a few decades.

The same lack of predictivity plagues also the neutralino detection rates, as shown in the scatter plot of Fig.2, in the case of event rates for direct detection. Again, supersymmetric models, only constrained by accelerators limits, are unable to provide definite predictions. However, it is remarkable that the scatter plot, which displays the range of the theoretical expectations, constrained here exclusively by bounds from accelerators (see Sect. III for details on the theoretical model employed), expands into the region of the current experimental sensitivity, i.e. above the experimental upper bound [10] denoted by the solid curve. Indeed, the significant improvements achieved in the sensitivity of the experiments of WIMP direct search in recent years, enable these experimental means to explore supersymmetric configurations which are simultaneounsly being investigated at accelerators [11].

Most remarkably, recent measurements performed by the DAMA Collaboration [12,13,14], have provided an indication of an annual modulation effect [15,16] (which is at present the unique, experimentally accessible way to disentangle an effect due to WIMPs from the background). Indeed, no plausible background appears to be able to mimick a time dependance of the sort singled out by the DAMA experiment. Thus the measured annual modulation effect (at a 99.6 % C.L.), reported in Refs. [12,13,14], if confirmed by further statistics, would be a major breakthrough in the dark matter issue. These experimental results have prompted theoretical investigations in terms of relic neutralinos in Refs. [17,18,19,20], where it has been proved that: i) the DAMA annual modulation data are compatible with a neutralino as a major component of dark matter in the universe, ii) a significant number of the relevant supersymmetric configurations are compatible with supergravity schemes [19], and iii) are explorable at accelerators and/or by indirect searches for relic particles (up-going muons at neutrino telescopes and antiprotons in space) [20]. Analyses of the DAMA results in the framework of SUGRA models have also been carried out in Refs. [22,23].

In the present paper we report some results of an extended analysis of the DAMA annual modulation data, with their implications in the framework of relic neutralinos [24]. Here our starting point is a DAMA region which is expanded as compared to the

one presented in Ref. [14], due to the effect of uncertainties in the relevant astrophysical velocities. The results summarized here are discussed in detail in Ref. [24], to which we refer for a thorough presentation; some of them were already preliminarily mentioned in Ref. [25].

2. Annual–modulation region

The spectrum dR/dE_R which is measured in WIMP direct detection is related to the WIMP-nucleus differential cross–section $d\sigma/dE_R$ and to the WIMP velocity distribution by the expression

$$\frac{dR}{dE_R} = N_T \frac{\rho_\chi}{m_\chi} \int_{v_{\rm min}}^{v_{\rm max}} d\vec{v}\, f(\vec{v})\, v \frac{d\sigma}{dE_R}(v, E_R)\,, \tag{2}$$

where N_T is the number of the target nuclei per unit of mass, ρ_χ is the local WIMP density, $\vec{v}$ and $f(\vec{v})$ denote the WIMP velocity and velocity distribution function in the Earth frame ($v = |\vec{v}|$). The nuclear recoil energy is given by $E_R = m_{\rm red}^2 v^2 (1 - \cos\theta^*)/m_N$, where θ^* is the scattering angle in the WIMP–nucleus center–of–mass frame, m_N is the nuclear mass and $m_{\rm red}$ is the WIMP–nucleus reduced mass. The velocity $v_{\rm min}$ is defined as $v_{\rm min} = (m_N E_R / 2m_{\rm red}^2)^{\frac{1}{2}}$ and $v_{\rm max}$ is the maximal (escape) WIMP velocity in the Earth reference frame. Eq.(2) refers to a mono-atomic detector; the generalization to our case of NaI is straightforward.

Since it turns out that in the WIMP-nucleus cross–section the coherent part is largely dominant over the spin–dependent one in almost the entire supersymmetric parameter space, we simply write dR/dE_R directly in terms of the scalar WIMP-nucleon cross–section $\sigma_{\rm scalar}^{\rm (nucleon)}$ as

$$\frac{d\sigma}{dE_R} = \left(\frac{1 + m_\chi/m_p}{1 + m_\chi/m_N} \right)^2 \frac{F^2(q)}{E_R^{\rm max}}\, A^2\, \sigma_{\rm scalar}^{\rm (nucleon)}, \tag{3}$$

where $E_R^{\rm max}$ is the maximum value of E_R, $F(q)$ denotes the nuclear form factor, expressed as a function of the momentum transfer $q^2 \equiv |\ \vec{q}\ |^2 = 2 m_N E_R$, m_p is the proton mass and A is the mass number of the nucleus. The nuclear form factor may very reliably be expressed in terms of the Helm parametric form [26,11].

To extract the quantity $\rho_\chi \sigma_{\rm scalar}^{\rm (nucleon)}$ as a function of m_χ from the measured spetrum dR/dE_R, one has to assume a functional form for the velocity distribution $f(v)$ and to assign appropriate values to its parameters [27]. Here, we make the usual assumption that in the galactic rest frame the WIMP velocities follow a Maxwell–Boltzmann distribution with a rms speed given by $v_{\rm rms} = \sqrt{\frac{3}{2}} v_\infty$ (with $v_\infty \simeq v(r_\odot) \equiv v_0$), and a finite escape velocity v_{esc}. Transformation from the galactic rest frame to the Earth rest frame, as required to make use of Eq. (2), is performed by taking into account that the Earth moves through the Galaxy with a velocity

$$v_\oplus = v_\odot + v_{\rm orb}\ \cos\gamma\ \cos[\omega(t - t_0)], \tag{4}$$

in the azimuthal direction. $v_\odot$ is given by

$$v_\odot = v_0 + 12\ {\rm km\ s^{-1}}. \tag{5}$$

In these expressions the speed of 12 km s^{-1} stands for the motion of the Solar System with respect to the Local System, $v_{\rm orb} = 30$ km s^{-1} denotes the Earth orbital speed around the Sun, the angle $\gamma \simeq 60^0$ is the inclination of the Earth orbital plane with respect to the galactic plane and $\omega = 2\pi/365$days, $t_0 =$ June $2^{\rm nd}$ [15,16].

We give in Fig.3 the (2–σ C.L.) annual–modulation regions extracted from the DAMA/NaI data of Ref. [14] (total exposure of 19,511 kg $\times$ day) for sets of values for v_0 and $v_{\rm esc}$, which bracket their physical ranges [28,29,30]:

$$v_0 = (220 \pm 50) \text{ km s}^{-1} \ \ (90\% \text{ C.L.}) \,, \tag{6}$$

$$v_{\rm esc} = (450 \div 650) \text{ km s}^{-1} \ \ (90\% \text{ C.L.}) \,. \tag{7}$$

¿From the features displayed in Fig.3 it appears that, as expected on general grounds [24]: i) the location of the annual–modulation region is rather sensitive to the velocity v_0, with a sizeable extension in the range of m_χ, but with small variations in $\rho_\chi \sigma^{\rm (nucleon)}_{\rm scalar}$; ii) the annual–modulation region is essentially independent of $v_{\rm esc}$.

The range of m_χ (at 1–σ C.L.) turns out to be

$$30 \text{ GeV} \lesssim m_\chi \lesssim 130 \text{ GeV} \,. \tag{8}$$

The annual–modulation region which takes into account the whole ranges of v_0 and $v_{\rm esc}$ (hereafter referred to as region R_m) is the one displayed by a closed contour in Fig.4.

We remark here that the dark matter halo could be affected by a bulk rotation, whose effect would be to extend the previously derived region R_m. Unfortunately, halo models capable of taking into account this effect realistically are not yet available; however, an evaluation may be carried out in a class of extreme models [31], which were already employed to study effects on direct detection rates [32,33] and on the ensuing upper bounds on the neutralino-nucleon cross–section [33]. In this framework, and allowing for physical values of the dimensionless galactic angular momentum [34], one finds the enlarged annual–modulation regions displayed in Fig.5 and the following range (at 1–σ C.L.) for m_χ

$$30 \text{ GeV} \lesssim m_\chi \lesssim 180 \text{ GeV} \,. \tag{9}$$

A bulk dark matter rotation is an intriguing possibility which should be further investigated with more realistic halo models. In the present paper, as far as implications in terms of neutralinos are concerned, we focus our analysis on the region R_m previously defined.

3. Implications for relic neutralinos

Let us turn now to the interpretation of the annual modulation data in the framework of relic neutralinos. The theoretical supersymmetric model considered here is the Minimal Supersymmetric extension of the Standard Model (MSSM) [2] with the specifications given in Refs. ([18,24]). In our scheme, the independent susy parameters are: $M_2, \mu, \tan\beta, m_A, m_0, A$, where M_2 is the $SU(2)$ gaugino mass, μ is the Higgs–mixing parameter, $\tan\beta$ is the ratio of the two Higgs vacuum expectation values,

m_A is the mass of the neutral pseudoscalar Higgs boson, m_0 is the common value associated to all squarks and sleptons soft–mass parameters which are taken as degenerate, and A is the trilinear parameter of the third family. To get the scatter plots shown in this paper, the supersymmetric space has been randomly scanned with the parameters delimited by the following ranges: 10 GeV $\leq M_2 \leq$ 1000 GeV, 10 GeV $\leq |\mu| \leq$ 1000 GeV, 80 GeV $\leq m_A \leq$ 1 TeV, 100 GeV $\leq m_0 \leq$ 1 TeV, $-3 \leq A \leq +3$, $1 \leq \tan\beta \leq 50$.

Our supersymmetric parameter space is constrained by all the experimental limits obtained from accelerators on supersymmetric and Higgs searches, by the requirement that the neutralino is the LSP, and by the cosmological bound, which is conservatively set here as $\Omega_\chi h^2 \leq 0.7$. The neutralino relic abundance is calculated as in Ref.[35]; the instances under which coannihilation effects might be sizeable [36] are marginal for the supersymmetric configurations concerning the DAMA/NaI data.

The generic scatter plots given in Figs. 2 and 4 have been derived by evaluating the cross–section $\sigma_{\rm scalar}^{\rm (nucleon)}$ as illustrated in Ref. [18] and ρ_χ with the usual rescaling procedure. This rescaling consists in writing the neutralino local density as $\rho_\chi = \xi\rho_l$ (ρ_l is the total local density of non-baryonic dark matter), with $\xi = {\rm Min}\,(1,\ \Omega_\chi h^2/(\Omega h^2)_{\rm min})$. $(\Omega h^2)_{\rm min}$ is the minimal value of $\Omega\, h^2$, compatible with observational data and with large–scale structure calculations. The value of $(\Omega h^2)_{\rm min}$ is somewhat arbitrary, in the range $0.01 \lesssim (\Omega h^2)_{\rm min} \lesssim 0.2$. In the present paper, whenever we have to apply rescaling, we use the value $(\Omega h^2)_{\rm min} = 0.01$, which is conservatively derived from the estimate $\Omega_{\rm galactic} \sim 0.03$.

The most remarkable feature of Fig.4 is that the generic scatter plot covers a sizeable part of the region R_m, showing that the annual–modulation region previously derived is compatible with supersymmetric configurations currently allowed by accelerator constraints.

We proceed now to a study of the supersymmetric configurations which fall inside the region R_m. Some features pertaining only to their cosmological properties may be derived without any use of the rescaling procedure. We can proceed as illustrated in the second paper of Ref. [17], i.e. we evaluate $\sigma_{\rm scalar}^{\rm (nucleon)}$ and $\Omega_\chi h^2$ by varying the supersymmetric parameters over the susy space previously defined, then, for any value of $[\rho_\chi\sigma_{\rm scalar}^{\rm (nucleon)}]_{\rm expt}$ compatible with the region R_m, we calculate ρ_χ as given by $\rho_\chi = [\rho_\chi\sigma_{\rm scalar}^{\rm (nucleon)}]_{\rm expt}/\sigma_{\rm scalar}^{\rm (nucleon)}$, and restrict the values of m_χ to stay inside the region R_m displayed in Fig.4. As a result we obtain, for instance, the scatter plot of Fig.6. (for other values of $[\rho_\chi\sigma_{\rm scalar}^{\rm (nucleon)}]_{\rm expt}$ which bracket the experimental range of DAMA data, see Ref. [24]). The two horizontal lines delimit the physical range 0.1 GeV cm$^{-3} \leq \rho_l \leq$ 0.7 GeV cm^{-3} for the total local density of non–baryonic dark matter. This (rather generous) range has been established by taking into account a possible flattening of the dark matter halo [37,38] and a possibly sizeable baryonic contribution to the galactic dark matter [39]. The solid vertical lines delimit the cosmologically interesting range $0.01 \leq \Omega_\chi h^2 \leq 0.7$. The two vertical dashed lines delimit the range: $0.02 \leq \Omega_\chi h^2 \leq 0.2$, which represents the most appealing interval. Indeed, recent observations and analyses [40] favour $0.1 \lesssim \Omega_{\rm matter} \lesssim 0.4$. Combining this range with the one for h: $0.55 \lesssim h \lesssim 0.80$ [41] and requiring that a cold dark matter candidate (such as the neutralino) supplies $\sim$ (80–90)% of $\Omega_{\rm matter}$. The two slant dot–dashed

lines delimit the band where linear rescaling procedure for the local density is usually applied. The upper dot–dashed line would refer to a rescaling with $(\Omega h^2)_{\rm min} = 0.01$, the lower one to the value $(\Omega h^2)_{\rm min} = 0.2$.

A few comments are in order here: i) configurations whose representative points fall above the maximum value $\rho_\chi = 0.7$ GeV cm^{-3} have to be excluded; ii) configurations falling in the region inside both the horizontal and solid vertical lines are very appealing, since they correspond to a neutralino could have the role of a dominant cold dark matter component; even more so, if the representative points fall in the subregion inside the vertical band delimited by dashed lines; iii) configurations which fall inside the band delimited by the slant dot–dashed lines denote situations where the neutralino can only provide a fraction of the cold dark matter both at the level of local density and at the level of the average Ω; and, finally iv) configurations above the upper dot–dashed line and below the upper horizontal solid line would imply a stronger clustering of neutralinos in our halo as compared to their average distribution in the Universe.

We now address the question of the explorability of the supersymmetric configurations, whose representative points fall inside the region R_m (hereafter denoted as configurations of set S_m), by accelerators of the present generation.

The supersymmetric configurations of set S_m are constrained by the inequalities

$$\frac{[\rho_\chi \sigma_{\rm scalar}^{\rm (nucleon)}]_{\rm expt}}{\rho_{\chi,{\rm max}}} \leq \sigma_{\rm scalar}^{\rm (nucleon)} \leq \frac{[\rho_\chi \sigma_{\rm scalar}^{\rm (nucleon)}]_{\rm expt}}{\rho_{\chi,{\rm min}}} \tag{10}$$

where $\rho_{\chi,{\rm min}} = \xi \rho_{l,{\rm min}} = \xi \cdot 0.1$ GeV cm^{-3} and $\rho_{\chi,{\rm max}} = \xi \rho_{l,{\rm max}} = \xi \cdot 0.7$ GeV cm^{-3}, and $[\rho_\chi \sigma_{\rm scalar}^{\rm (nucleon)}]_{\rm expt}$ is any value inside region R_m as a function of m_χ.

We summarize in Figs. 7-9 the main correlations implied by Eq. (10) among the supersymmetric parameters. Fig.7 displays the scatter plot of $\tan\beta$ versus the mass m_h of the lightest neutral CP-even Higgs boson (m_h may be derived from the supersymmetric parameters listed above). From this figure it turns out that a number of supersymmetric configurations of set S_m could still be explorable at LEP2, but the others require investigation at a high luminosity Fermilab Tevatron [42,43] or at LHC. A correlation between $\tan\beta$ and the mass of the lightest top–squark $m_{\tilde{t}_1}$ is shown in Fig.8. Finally, Fig.9 gives the plot of $\tan\beta$ versus m_χ; a correlation shows up here for not too large values of $\tan\beta$. LEP2 can only provide an investigation up to $m_\chi \simeq 50$ GeV. The exploration up to ~ 125 GeV can be performed with Tevatron upgrades (under favorable conditions), while for higher values of m_χ LHC is needed.

4. Conclusion

In the present report we have first shown how the original DAMA/NaI annual–modulation region in the plane $\rho_\chi \sigma_{\rm scalar}^{\rm (nucleon)} - m_\chi$ [14] is extended when the uncertainties in the galactic astrophysical velocities are taken into account. Most remarkably, the range for the neutralino mass becomes 30 GeV $\lesssim m_\chi \lesssim$ 130 GeV at 1–σ C.L., with a further extension in the upper bound, when a possible bulk rotation of the dark matter halo is taken into account. We have then discussed the main properties of the supersymmetric configurations singled out by the DAMA/NaI data, proving that they have cosmological properties compatible with a relic neutralino as a dominant

component of cold dark matter (on the average in our universe and in our galactic halo). We have also examined the features of the relevant supersymmetric configurations in connection with the discovery potential of the accelerators of the present generation.

5. References

1) For a review on dark matter and its particle candidates, see for instance A. Bottino and N. Fornengo, Proceedings of the Fifth School on Non-Accelerator Particle Astrophysics at the Abdus Salam International Centre for Theoretical Physics (Eds. R.A. Carrigan, G. Giacomelli and N. Paver, to be published), *hep-ph/9904469*.
2) H.P. Nilles, Phys. Rep. **110**, 1 (1984); H.E. Haber and G.L. Kane, Phys. Rep. **117**, 75 (1985); R. Barbieri, Riv. Nuovo Cim. **11**, 1 (1988).
3) A. Bottino, F. Donato, F. Fornengo and P. Salati, Phys. Rev. **D58** (1998) 12503; L. Bergström, J. Edsjö and P. Ullio, *astro-ph/9902012*; J.W. Bieber, R.A. Burger, R. Engel, T.K. Gaisser, S. Roesler and T. Stanev, *astro-ph/9903163*.
4) F. Donato, N. Fornengo and P. Salati, *hep-ph/9904481*.
5) E.A. Baltz and J. Edsjö, Phys. Rev. **D59** (1999) 023511.
6) L. Bergström, P. Ullio and J. Buckley, Astrop. Phys. **9** (1998) 137.
7) L. Bergström, T. Damour, J. Edsjö, L.M. Krauss, P. Ullio, *hep-ph/9905446*.
8) However, expected neutrino oscillations in the signal (see Ref. [9]) should be taken into account and would somewhat attenuate the total neutrino flux.
9) N. Fornengo, Proceedings of the International Workshop "Weak Interactions and Neutrinos (WIN99)", Cape Town, South Africa, January 1999 (ed. Dominguez, Viollier), *hep-ph/9904351*.
10) R. Bernabei *et al.*, Phys. Lett. **B389** (1996) 757.
11) A. Bottino, F. Donato, G. Mignola, S. Scopel, P. Belli and A. Incicchitti, Phys. Lett. **B402** (1997) 113.
12) R. Bernabei *et al.*, Phys. Lett. B **424**, 195 (1998).
13) R. Bernabei *et al.*, University of Rome Report No. ROM2F/98/27 and INFN Report INFN/AE–98/23 available on *http://mercury.lngs.infn.it/lngs/preprint/preprint.html*, to appear on Nuovo Cimento *A*.
14) R. Bernabei *et al.*, Phys. Lett. **B450** 448, (1999).
15) A.K. Drukier, K. Freese and D.N. Spergel, Phys. Rev. D **33**, 3495 (1986).
16) K. Freese, J. Frieman and A. Gould, Phys. Rev. D **37**, 3388 (1988).
17) A. Bottino, F. Donato, N. Fornengo and S. Scopel, Phys. Lett. B **423**, 109 (1998), and *hep-ph/9710295*, Torino University Report No. DFTT 61/97 (unpublished).
18) A. Bottino, F. Donato, N. Fornengo and S. Scopel, Phys. Rev. D **59**, 095003 (1999).
19) A. Bottino, F. Donato, N. Fornengo and S. Scopel, Phys. Rev. D **59**, 095004 (1999).
20) A. Bottino, F. Donato, N. Fornengo and S. Scopel, Astropart. Phys. **10**, 203 (1999).

21) For an analysis of the DAMA/NaI annual–modulation data in supergravity unified models, see also R. Arnowitt and P. Nath, *hep-ph/9902237*.
22) R. Arnowitt and P. Nath, *hep-ph/9902237*.
23) A. Corsetti and P. Nath, *hep-ph/9904497 v2*.
24) P. Belli, R. Bernabei, A. Bottino, F. Donato, N. Fornengo, D. Prosperi and S. Scopel, *hep-ph/9903501*
25) N. Fornengo, *hep-ph/9812210*, *Proceeding of the International Workshop on the Identification of Dark Matter (IDM98), Buxton, 1998*, edited by N. Spooner (World Scientific, to appear).
26) R.H. Helm, Phys. Rev. D **104**, 1466 (1956).
27) The dependence of the WIMP detection rates on astrophysical velocities is a well known effect; it was for instance quantitatively discussed in Bacci *et al.*, Astrop. Phys. **2**, 117 (1994) and in Ref. [11]. The implications of this property for the DAMA modulation region was shown first at this conference in the talks by R. Bernabei and A. Bottino and anticipated in Ref. [25]. Similar considerations, though limited to the dependence on v_0, were subsequently also presented in *hep-ph/9903467* (by L. Roszkowski) and *hep-ph/9903468* (by M.Brhlik and L. Roszkowski). It should be noted that in *hep-ph/9903468* some of our results in Ref. [18] are erroneously reported.
28) P.J.T. Leonard and S. Tremaine, Astrophys. J. **353**, 486 (1990).
29) C.S. Kochanek, Astrophys. J. **457**, 228 (1996).
30) K.M. Cudworth, Astron. J. **99**, 590 (1990).
31) D. Lynden–Bell, Mon. Not. R. Astron. Soc. **120**, 204 (1960).
32) M. Kamionkowski and A. Kinkhabwala, Phys. Rev. D **57**, 3256 (1998).
33) F. Donato, N. Fornengo and S. Scopel, Astropart. Phys. **9**, 297 (1998).
34) S. Warren, P.J. Quinn, J.K. Salmon, W.H. Zurek, Astrophys. J. **399**, 405 (1992); S. Cole, C. Lacey, Mon. Not. R. Astron. Soc. **281**, 716 (1996).
35) A. Bottino, V. de Alfaro, N. Fornengo, G. Mignola and M. Pignone, Astropart. Phys. **2**, 67 (1994).
36) P. Binétruy, G. Girardi and P. Salati, Nucl. Phys. **B237**, 285 (1984); K. Griest and D. Seckel, Phys. Rev. **D43**, 3191 (1991); S. Mizuta and M. Yamaguchi, Phys. Lett. **B298**, 120 (1993); J. Edsjö and P. Gondolo, Phys. Rev. **D56**, 1879 (1997).
37) E. Gates, G. Gyuk and M.S. Turner, Phys. Rev. Lett. **74**, 3724 (1995); Phys. Rev. **D53**, 4138 (1996).
38) E. Gates, G. Gyuk and M.S. Turner, Astrophys. J. Lett. **449**, L123 (1995).
39) E. Gates, G. Gyuk and M.S. Turner, *astro-ph/9704253*, *Proceedings of the 18th Texas Symposium on Relativistic Astrophysics*, edited by A. Olinto, J. Frieman and D. Schramm (World Scientific, to appear).
40) W.L. Freedman, R. Kirshner and C. Lineweaver, talks given at the International Conference of Cosmology and Particle Physics (CAPP98), CERN, June 1998, *wwwth.cern.ch/capp98/programme.html*; M. White, Astrophys. J. **506**, 495 (1998); N.A. Bahcall and X. Fan, *astro-ph/9804082* to appear in National Academy of Sciences Proc.; C. Lineweaver, *astro-ph/9805326*, (to appear in Astrophys. J. Lett.).
41) A. Sandage *et al.*, Astrophys. J. Lett. **460**, L15 (1996); W. L. Freedman, *astro-ph/9706072*, *Proceedings of the 18th Texas Symposium on Relativistic*

Astrophysics, edited by A. Olinto, J. Frieman and D. Schramm (World Scientific, to appear). and references quoted therein.
42) Report of the TeV–2000 Study Group, edited by D. Amidei, R. Brock, Fermilab Report No. FERMILAB–PUB–96/082, 1996.
43) H. Baer, B.W. Harris and X. Tata, Florida State University Phys. Rev. D **59** 015003 (1999).

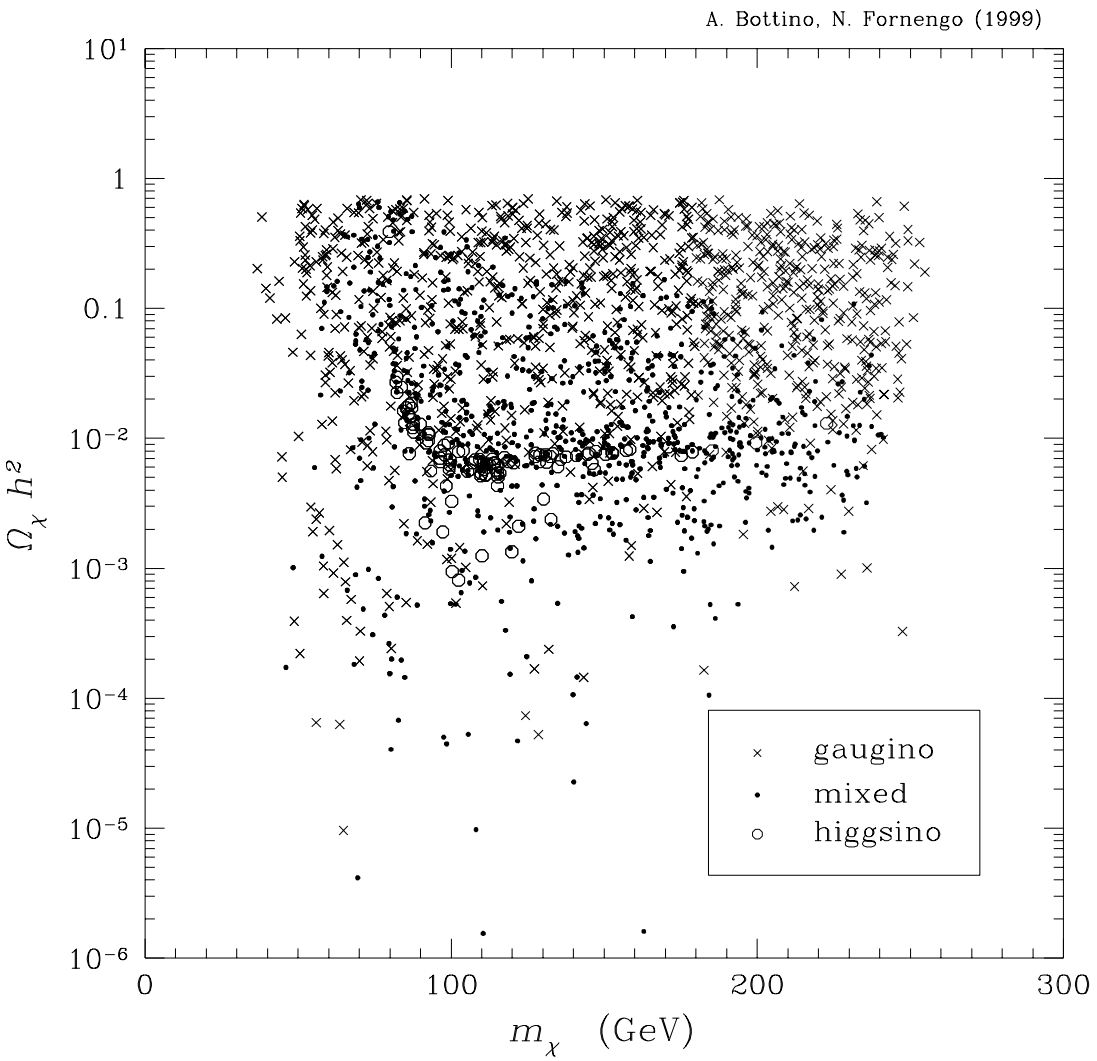

FIG. 1. Scatter plot of the neutralino relic abundance as a function of the neutralino mass.

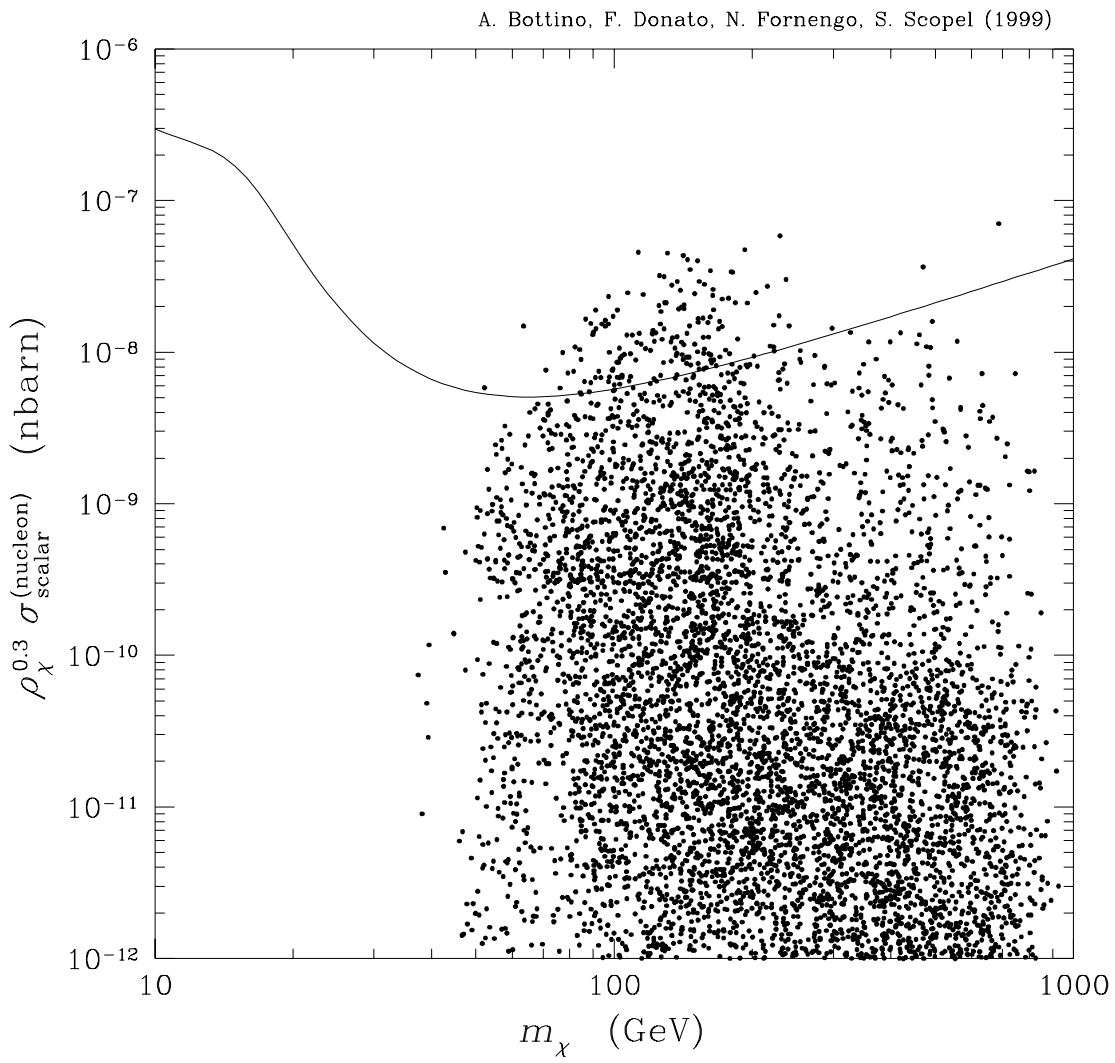

FIG. 2. Scatter plot of the neutralino local density times the neutralino–nucleon scalar cross–section as a function of the neutralino mass. The quantity $\rho_\chi^{0.3}$ is the local neutralino matter density in units of 0.3 GeV cm^{-3}. The solid line denotes the experimental upper bound of Ref. [10].

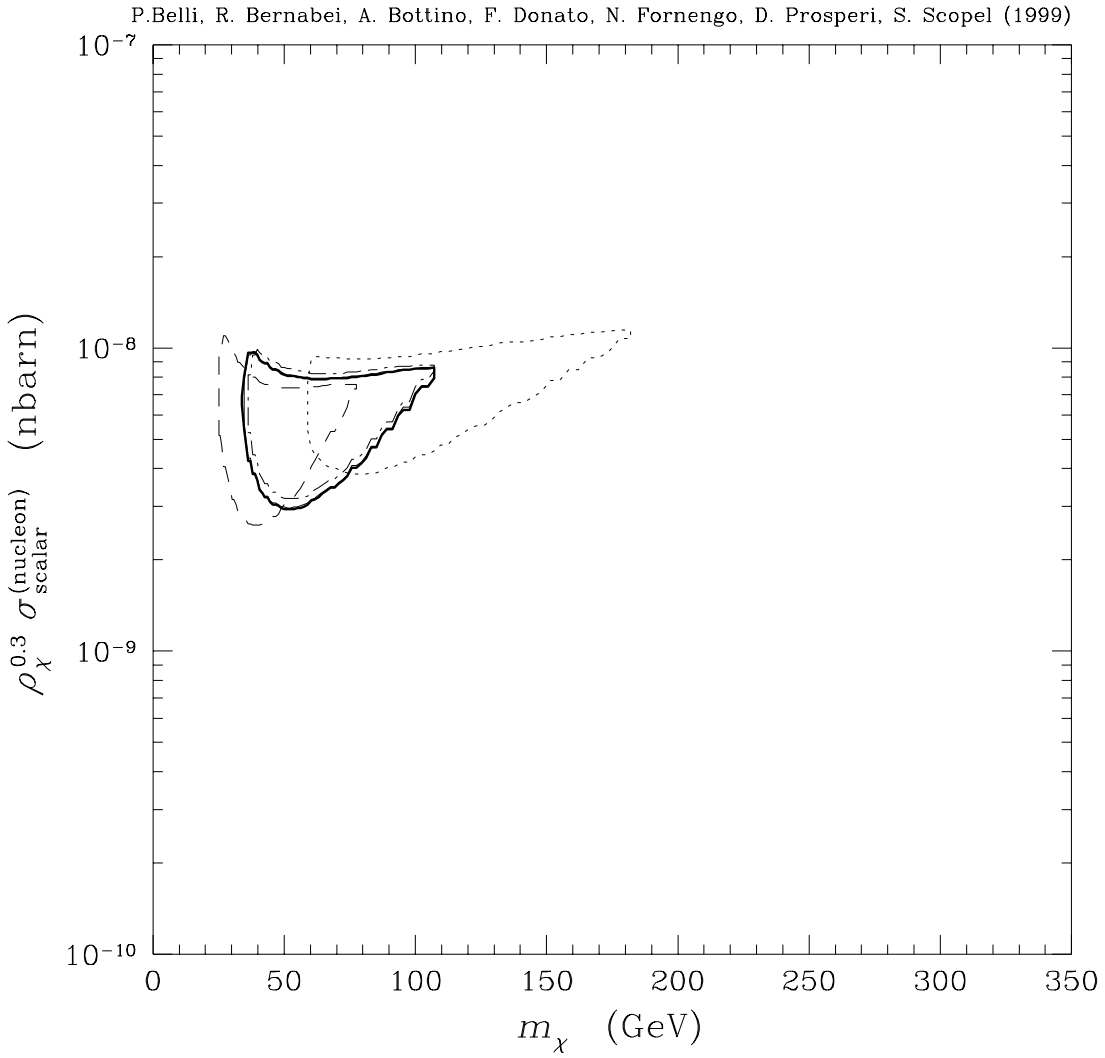

FIG. 3. Annual–modulation regions singled out by the DAMA/NaI experiment [12] in the plane $\rho_\chi^{0.3}\sigma_{\rm scalar}^{\rm (nucleon)} - m_\chi$ for various values of velocities v_0 and v_{esc}: $v_0 = 220$ km s^{-1}, $v_{esc} = 650$ km s^{-1} (solid line); $v_0 = 220$ km s^{-1}, $v_{esc} = 450$ km s^{-1} (dot–dashed line); $v_0 = 170$ km s^{-1}, $v_{esc} = 550$ km s^{-1} (dotted line); $v_0 = 270$ km s^{-1}, $v_{esc} = 550$ km s^{-1} (dashed line). The countour line for $v_0 = 220$ km s^{-1}, $v_{esc} = 550$ km s^{-1} is indistinguishable on the plot from the solid line. The quantity $\rho_\chi^{0.3}$ is the local neutralino matter density in units of 0.3 GeV cm^{-3}.

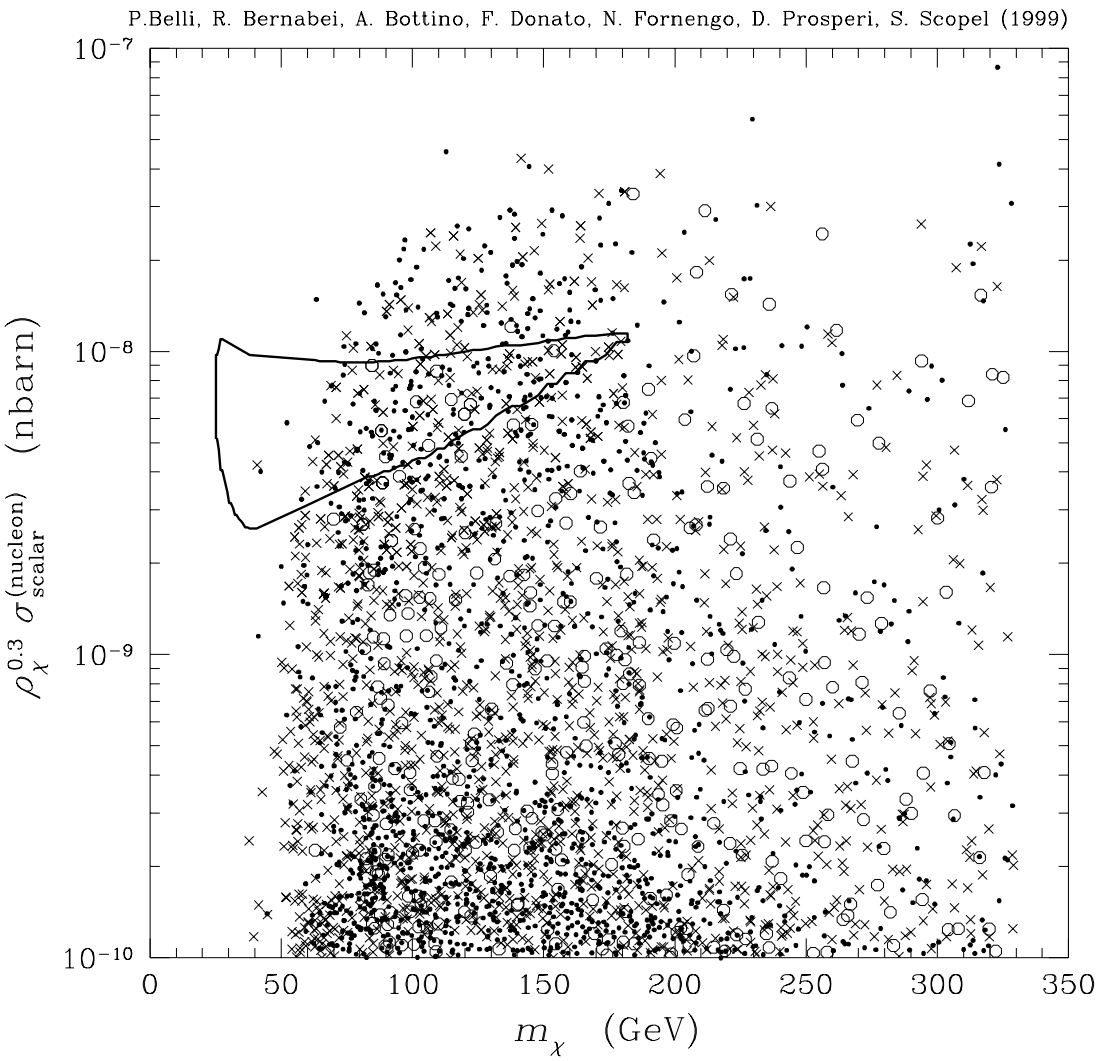

FIG. 4. The contour line delimits the annual–modulation region obtained by varying the velocities v_0 and v_{esc} over the ranges given in Eqs. (6 – 7). The scatter plot represents the theoretical predictions of a generic MSSM, as described in Sect. III. Different symbols identify different neutralino compositions: circles stand for a higgsino, crosses for a gaugino and dots for a mixed neutralino. The quantity $\rho_\chi^{0.3}$ is the local neutralino matter density in units of 0.3 GeV cm^{-3}.

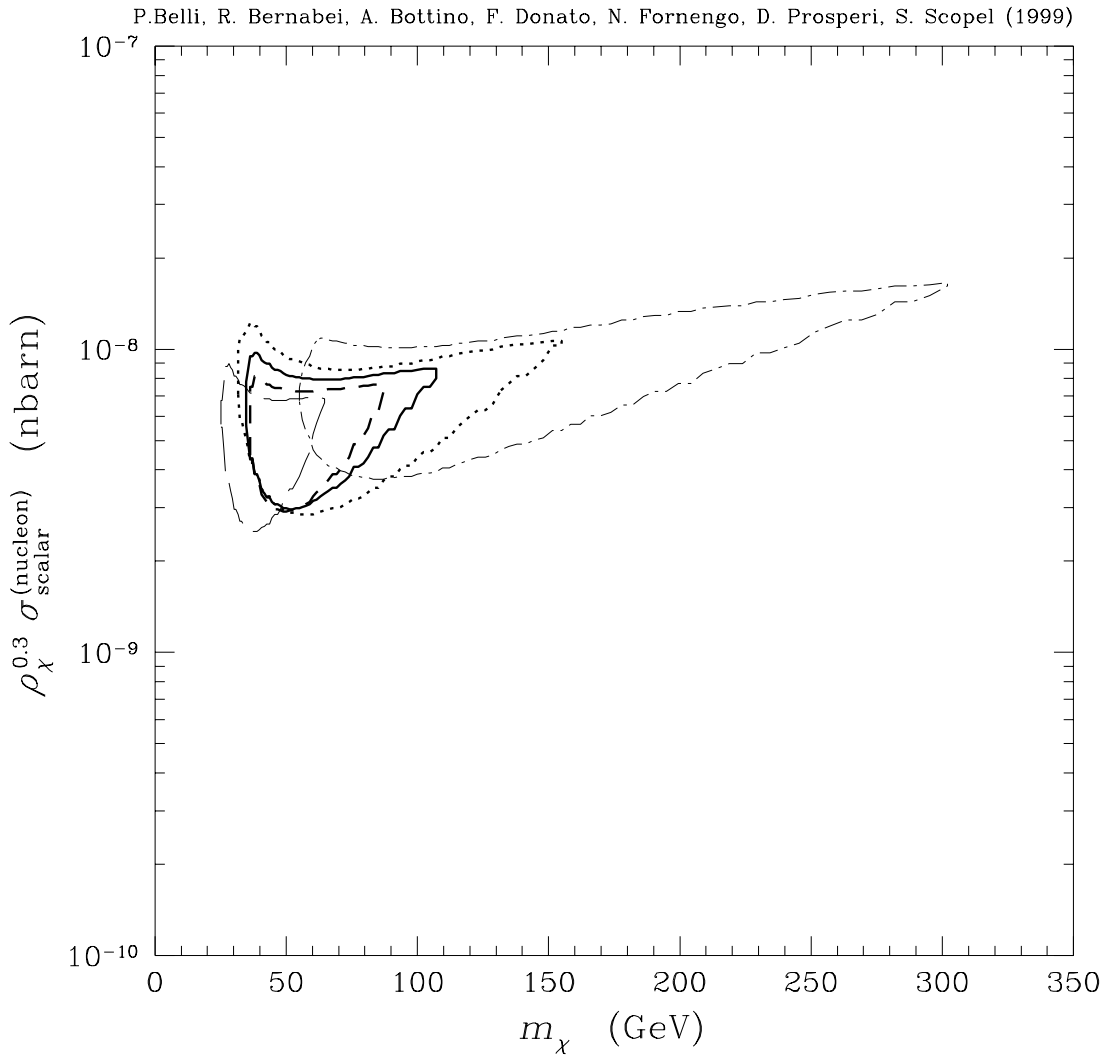

FIG. 5. Annual–modulation regions when a possible bulk rotation of the dark matter halo is taken into account. The contour lines refer to the following halo parameters: $v_0 = 220$ km s^{-1}, non rotating halo (solid line); $v_0 = 220$ km s^{-1}, co–rotating halo with spin parameter $\lambda = 0.05$ (dotted line); $v_0 = 220$ km s^{-1}, counter–rotating halo with $\lambda = 0.05$ (dashed line); $v_0 = 170$ km s^{-1}, co–rotating halo with $\lambda = 0.05$ (dot–dashed line); $v_0 = 270$ km s^{-1}, counter–rotating halo with $\lambda = 0.05$ (long–dashed line); The escape velocity is fixed at the value $v_{esc} = 550$ km s^{-1} for all the contours.

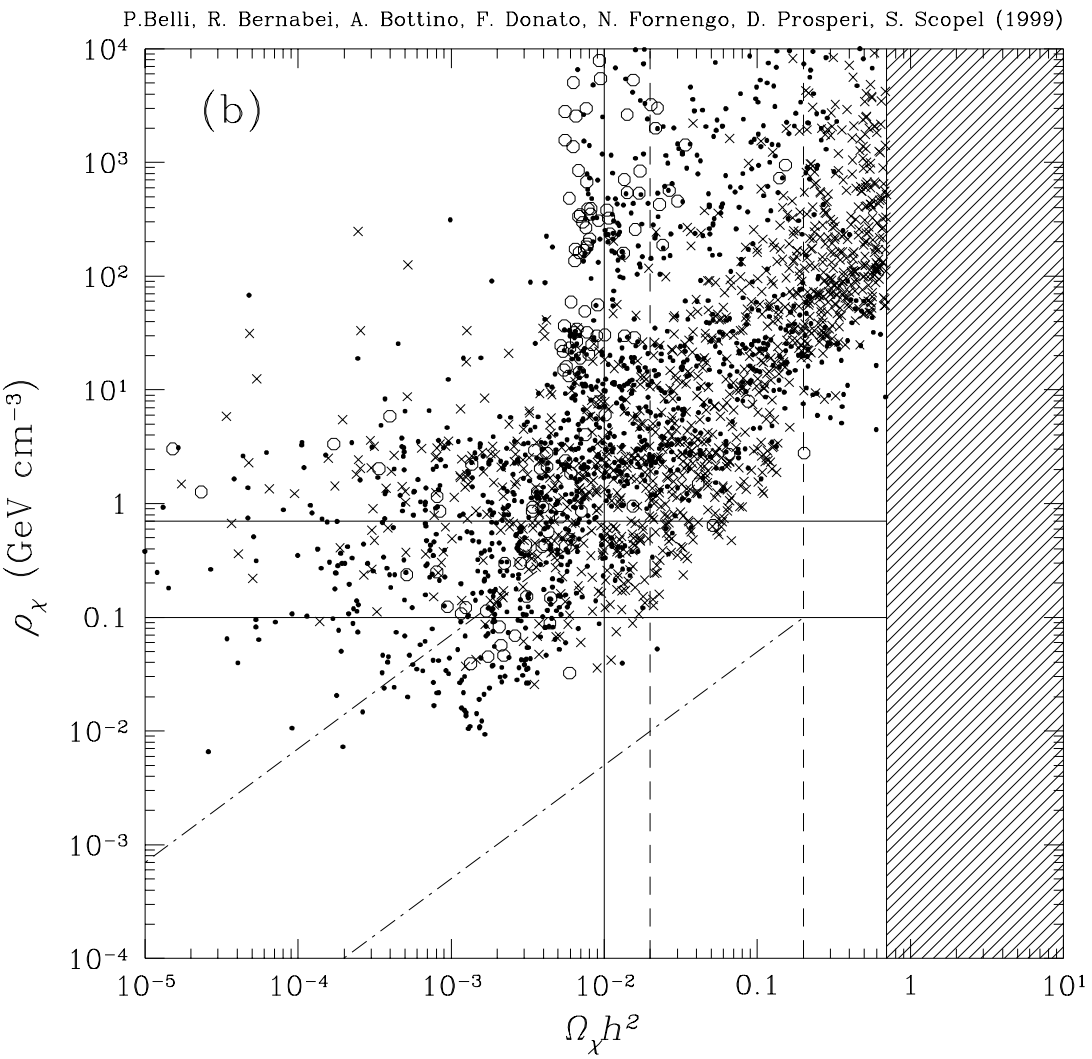

FIG. 6. The neutralino local density ρ_χ, calculated for the value $[\rho_\chi^{0.3}\sigma_{\rm scalar}^{\rm nucleon}]_{expt}$= $6 \cdot 10^{-9}$ nbarn and 25 GeV $\leq m_\chi \leq$ 131 GeV. The two horizontal lines delimit the physical range for the local density for non-baryonic dark matter. The two solid vertical lines delimit the interval of $\Omega_\chi h^2$ of cosmological interest. The two vertical dashed lines delimit the preferred band for cold dark matter. The two slant dot–dashed lines delimit the band where linear rescaling procedure is usually applied. Different symbols identify different neutralino compositions: circles stand for a higgsino, crosses for a gaugino and dots for a mixed neutralino.

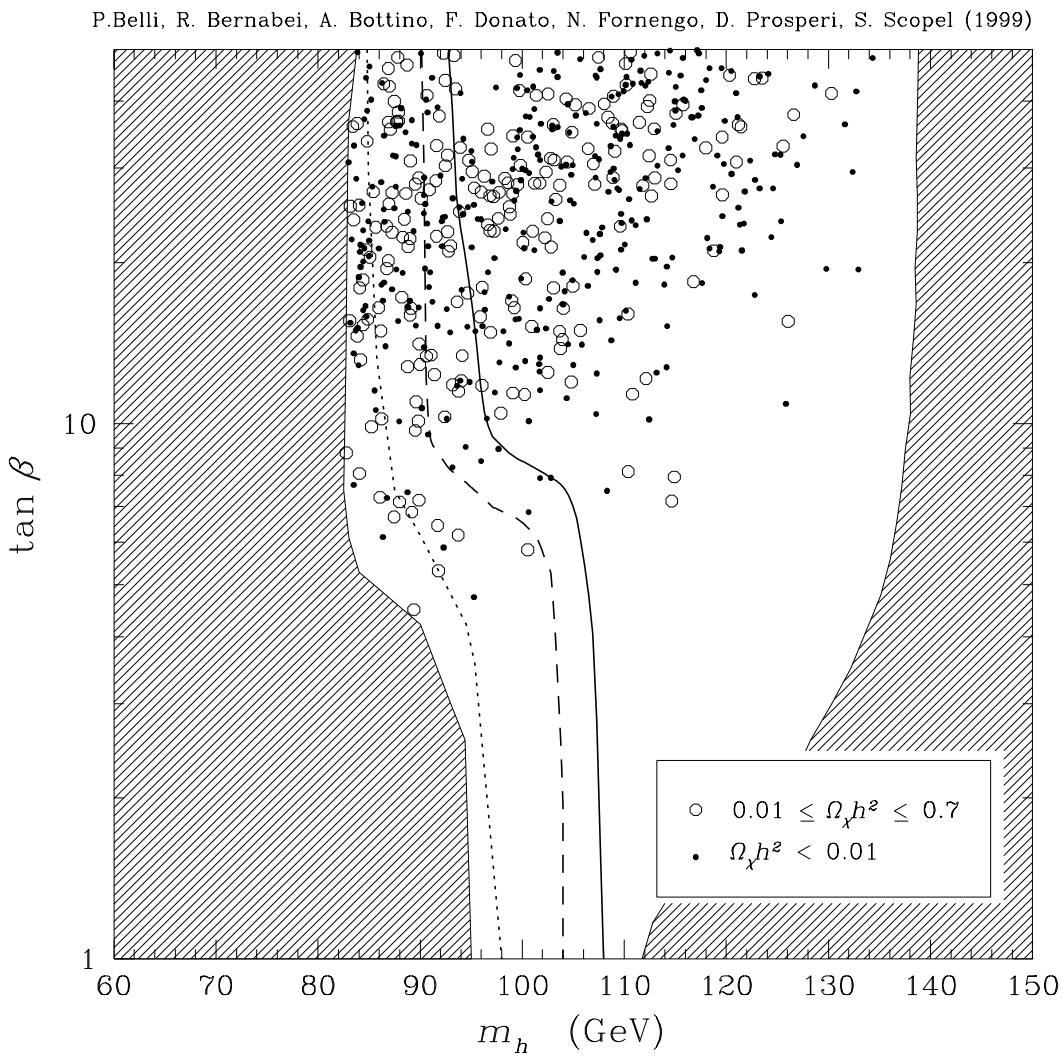

FIG. 7. Scatter plot for set S_m in the plane m_h – $\tan\beta$. The hatched region on the right is excluded by theory. The hatched region on the left is excluded by present LEP data at $\sqrt{s} = 189$ GeV. The dotted and the dashed curves denote the reach of LEP2 at energies $\sqrt{s} = 192$ GeV and $\sqrt{s} = 200$ GeV, respectively. The solid line represents the 95% C.L. bound reachable at LEP2, in case of non discovery of a neutral Higgs boson.

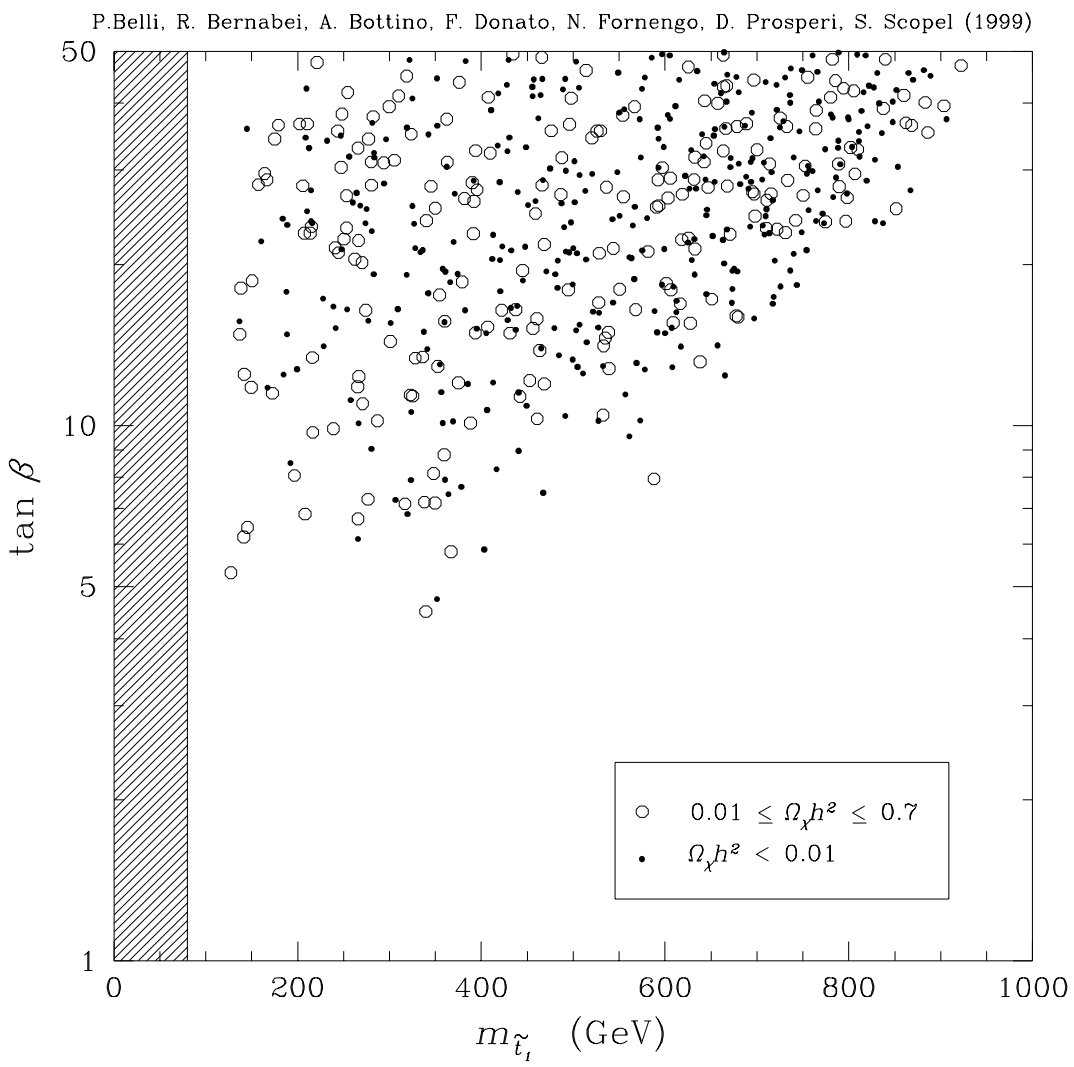

FIG. 8. Scatter plot for set S_m in the plane $m_{\tilde{t}_1}$ – $\tan\beta$. The hatched region is excluded by LEP data.

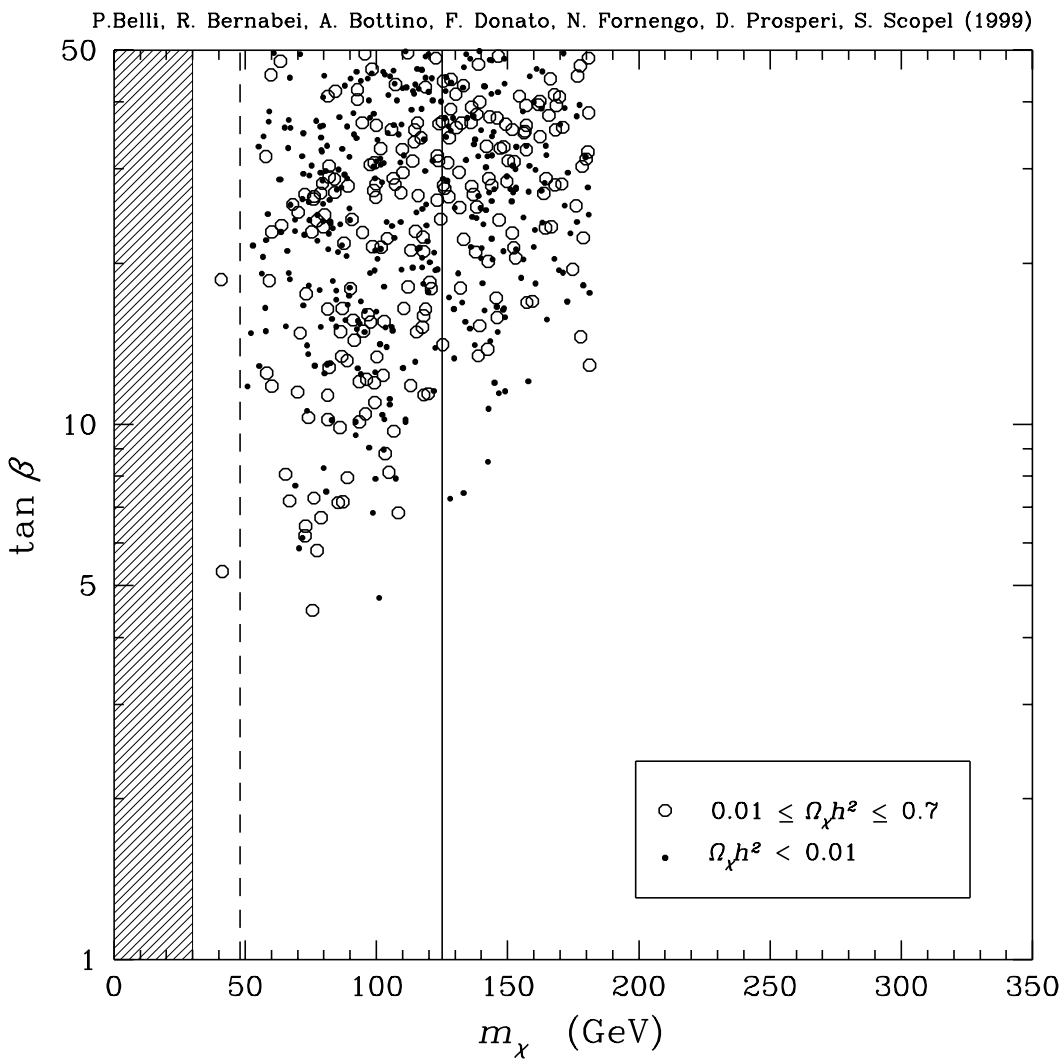

FIG. 9. Scatter plot for set S_m in the plane m_χ – $\tan\beta$. The hatched region on the left is excluded by present LEP data. The dashed and the solid vertical lines denote the reach of LEP2 and TeV33, respectively.